

Model development of bond graph based wind turbine

Sugiarto Kadiman, Oni Yuliani

Department of Electrical Engineering, Faculty of Engineering and Planning, Institut Teknologi Nasional Yogyakarta,
Yogyakarta, Indonesia

Article Info

Article history:

Received Sep 7, 2023

Revised Nov 25, 2023

Accepted Dec 9, 2023

Keywords:

20-Sim software

Bond graph

Doubly-fed induction generator

Torque control

Variable speed

ABSTRACT

Just recently, wind energy continues to be one of most important renewable energy resources, by cause of its production is ecologically friendly; for that reason, the technology built for the renewable energy production by way of wind turbines takes excessive challenges in the study. Due to several physical domains prevailing in wind turbine, namely aerodynamical, mechanical and electrical, the modeling of wind turbine is problematic; thus, modeling based on physical techniques has a superior reliability in these circumstances. One of these approaches is bond graph modeling that model system evolved from conservation law of both of mass and energy comprising in the structures. This study presents modeling the parts of bond graph-based wind turbine. Then, sub models are connected together to attain the entire model of wind turbine for simulation based on 20-Sim software. The proposed wind turbine is 2.5 kW of variable velocity wind turbine with three blades, gearbox, tower, and doubly-fed induction generator type. The effectiveness of bond graph modeling system on wind turbine has been proven in simulation results.

This is an open access article under the [CC BY-SA](#) license.



Corresponding Author:

Sugiarto Kadiman

Department of Electrical Engineering, Faculty of Engineering and Planning

Institut Teknologi Nasional Yogyakarta

Babarsari, Caturtunggal, Sleman, Yogyakarta, Indonesia

Email: sugiarto.kadiman@itny.ac.id

1. INTRODUCTION

Wind energy technology alongside renewable energy resources has seemed remarkably magnificent sources of power because of its affordability on the subject of economic gains and ecological friendliness [1]–[3]. Outstanding enhancement in the wind power design have been accomplished on account of modern technological developments in various aspects, namely expertise to produce the wind power effectually, growing quantity of wind energy facility and its growth from aground to isolated places and seaward. The progress continued somewhat affected through escalating demand of wind energy over the span of years. Nevertheless, the discontinuous characteristic of these reserves stays on substantial task in making dependable and continuing green energy network [4]–[6]. This problem has pictured the attention of researchers headed for cutting edge to create suitable solutions. A huge part of the developed solutions is established through typical of wind turbine structures. Their typical structures turn out to be an important draw a part of the discourse.

During couple years it existed a number of discourses concerning modelling of wind turbine precisely. Several researches conduct the dynamic analysis of model wind turbine using one-mass model [7], [8]. Some researchers examine a two-mass model [9], [10]. Meanwhile, other researchers use actual evaluated parameters from wind turbine and assess it by both of one mass and two mass configurations [11]. Proving the model is carried out through evaluation of under constant wind speed conditions and interrupt-controlled

system. Muyeen *et al.* [12] a two, three, and a six-mass scheme of wind turbine are competed. The results are revealed that a six-mass scheme is necessity for an accurate examination of wind turbine. The whole studies emphasize the significance of possessing a correct form of wind turbine, as a means of overseeing compelling examines of saying methods.

Wind turbine system is a many fields and multifaceted structure that dissimilar methodological topics are elaborated, such as aerodynamic, mechanical, and electrical. However, utilizing different methods earlier established. The intricacy of a wind turbine can be visualized although different methods for their applications. Beneath these circumstances, taking into consideration to investigate the system in identical coordinate system, the procedures of bond graph are able to describe every entire configuration [13]–[15]. This procedure offers some properties that can be implemented at first hand.

The bond graph comprises of components connected collectively by means of power connections. The instant power is replaced by the side of ports. The parameters that are put with interchangeable during connecting process between two ports as the power variables, regard as functions of time. The distinctive power parameters are categorized in general outline, and are termed any effort $e(t)$ or flow $f(t)$. The result $P(t)=e(t)\times f(t)$ is transitory power delivering between ports. Foremost advantages of the bond graph tool for forming objectives are a integrated graphical expression means to describe through bodily perception power exchanges, each energy depletion and energy storing phenomena in vigorous systems of every bodily field and also the picturing instrument of causality possessions for inscription equivalences corresponding in the direction of designated modeling premises.

The model of bond graph-based wind turbine can be obtained in numerous studies [16]–[18]. The comprehensive blade representation exists at the outset. The flowing intensity are counted. For the purpose to calculate the output power and blade behaviour, actual information of wind turbine put in application. Moreover, just the same a generic example that suitable to each wind turbine. Fu *et al.* [19], a comprehensive wind turbine depend on actual parameters is proposed. Every exemplary describes entire sections of the system excluding aerodynamics. This research undertakes wind turbine geared systems in hybrid randomness which appropriately to monitor the condition.

Recently, lots of the equipped wind turbines have retained the structure working with a gearbox. Rotated around this situation, a model of the gearbox is utilized as a means to complete the entire structure. Regarding bond graph procedure, gears are designed to be used in transmission system [20]. A comprehensive examination of pictorial apparatuses for modeling gears is specified [21]. All results reveal that bond graph procedure takes important attributions in comparison to everyone else. Gearbox is the headmost section of a wind turbine. At that section, most of misconducts are happened.

Many wind turbines use an induction machine to work as generator, yet some more synchronous machines have been appeared. Aimed at an induction machine, distinct assemblies have been utilized. A squirrel cage induction machine is implemented as a means to permit affluent joining to outward power grid and taking wind turbine deprived of electronics converters necessary in the rest structures. Occasionally a doubly-fed or wound rotor induction machine is presented because it is able to control the frequency and voltage due to wind speed changed. It also brings the advantage of utilizing the displacement ratio of the machine, so that the converter does not need to be rated for the full engine rating. In this study a model of bond graph-based wind turbine has three blades, gearbox, tower, and doubly-fed induction generator (DFIG) type, and which involves real data of 2.5 kW wind turbine [22]. Framework of this study is just when follows: at first, the wind turbine model is evolved. Then, complete kind is simulated based on 20-Sim software. Next section describes result and analysis. Finally, conclusions of the study are drawn.

2. SYSTEM DESCRIPTION

Figure 1 describes common structure of wind energy transfer approach. Variable velocity wind turbines can undertake maximum energy transfer usefulness around wide-reaching of wind velocity. The turbine can constantly adapt its rotational speed conferring to wind velocity. Thus, the tip velocity ratio that is fraction between blade tip velocity and wind velocity can be hold on to a best rate to accomplish ultimate energy conversion efficiency on varying wind velocities. Each individual section, namely blades, hub, gearbox, tower, and a doubly-fed induction generator, related to wind turbine structure in Figure 1, is combined through a bond. In almost all components are present an accompanying mechanical power, then the former segment which is generator converts mechanical power becomes electric power, signified in three bonds.

The power flow in wind turbine is rendering to bonds direction. Blades create bulky torque and is moved to gearbox through main shaft. Then, the gearbox transforms the bulky torque to small one to be utilized to the induction generator. A analogous condition is justifiable for rotational speed, such as fast-moving gave for generator. Gearbox converted fast-moving into a small speed, attainable at rotor turbine or hub.

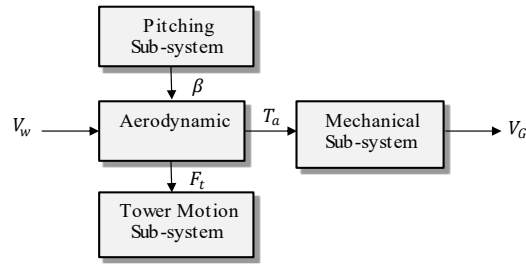


Figure 1. Variable speed wind turbine systems

2.1. Turbine blade model

The blade model is held on [23], shown in Figure 2. The study confirms that the blade construction signifies a universal representation. Consequently, wind turbines of various powers capacities are able to be act out using data conversion. The blade is split up into three sections or more.

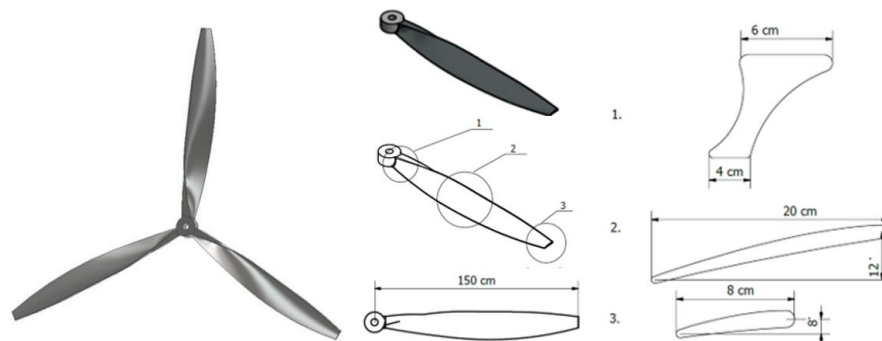


Figure 2. Blade form of wind turbine

2.1.1. Model structure

All physical model of the blade is constructed on Rayleigh beam form [24] and blade element momentum (BEM) principle [25]. Therefore, a dynamic form in the course of structural testing-based simulation can be made. These methods conform the blade as stiffness frame dynamics where its sections are basically dispersed structure frameworks, managed by partial differential calculation, and are massed in distance by finite elements, is shown in Figure 3. Every section has own displacement and this movement can be expressed as generalized Newton forces and displacements. Figure 4 shows the *i*-th section. The governing equations are

$$[F_1 \quad M_1 \quad F_2 \quad M_2]^T = [K_i][y_1 \quad \theta_1 \quad y_2 \quad \theta_2]^T \tag{1}$$

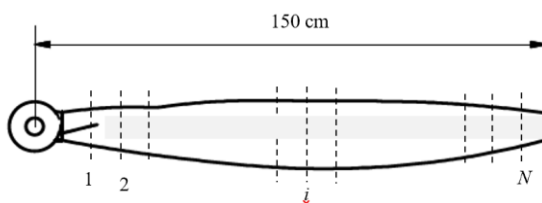


Figure 3. *N*-sections of blade

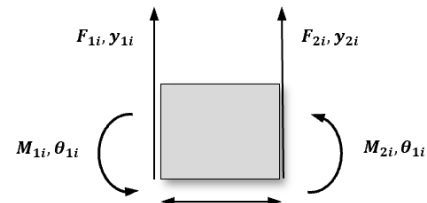


Figure 4. Beam with force and displacement

2.1.2. Aerodynamic force

In the realm of aerodynamics, it is required developing a method to turn wind into both of torque and thrust force, namely transforming a flow into an effort. The aforementioned is managed applying a modulated gyrator. Anderson [26], the equation of power created as a result of wind is specified by;

$$P = \frac{1}{2} \rho v^3 \pi R^2 C_p \tag{2}$$

where measureless tip speed ratio (TSR) λ is described by way of $\lambda = v_b/v$. The v_b is the tip of blade and v is wind velocity. From (2), it can be found both of an aerodynamic thrust force Q and torque T as;

$$Q = \frac{1}{2} \rho v^2 \pi R^3 (C_p/\lambda) \quad T = \frac{1}{2} \rho v^2 \pi R^2 C_v \tag{3}$$

where ρ and R denote air density and is the range of blade, respectively. Then, C_p represents power coefficient and C_v denotes the connection among existed power in the wind and value which transformed to electric power. At most distinction among modulated gyrator (MGY) and gyrator (GY) is that gyrator proportion is not a constant but fluctuating parameter. The conversion is determined on two of varying parameters, namely pitch angle β and rotor revolving velocity ω_r as shown in Figure 5.

Common equation is utilized to pattern the C_p . Equation form and its coefficients regarding turbine features is shown in (5) and (6). The chart of the C_p curve is displayed in Figure 6; a chart is created through dissimilar pitch and λ rates.

$$\lambda = \omega_r R / v \quad \lambda_i = 1 / (1 / (\lambda + 0.08\beta) - (0.035 / (\beta^2 + 1))) \tag{4}$$

$$C_p = C_1 ((C_2 / \lambda_i) - C_3 \beta - C_4) C^{C_5 / \lambda_i} + C_6 \lambda \tag{5}$$

with $C_1 = 0.5176$, $C_2 = 116$, $C_3 = 0.4$, $C_4 = 5$, $C_5 = 21$, and $C_6 = 0.0068$.

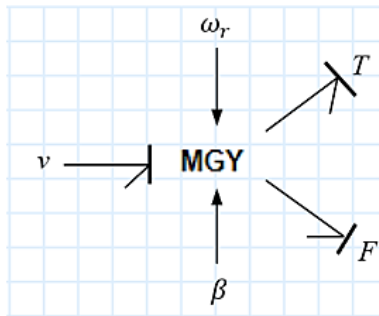


Figure 5. Modulated gyrator

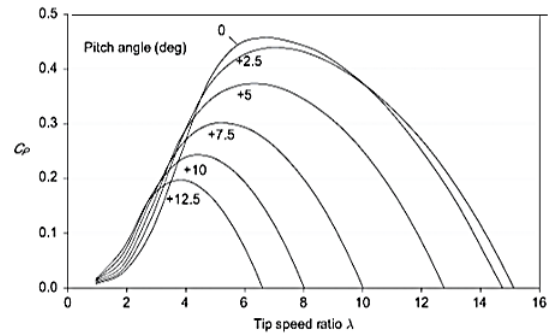


Figure 6. Effect pitch change on C_p [26]

The beam section based on bond graph is shaped by massing part inertias on center of gravity of the sections and linking it to the I -junctions characterizing movements and revolutions at the center of gravity of the element. The turbine blade assembly is created by means of C -field and R -field elements, that characterize both the rigidity and the physical absorbing mode between the center of gravity of nearby sections. The borderline form of the model is described between $S_f = V_{bound}$ and S_e sources. Connection among blade and hub is presumed to be stiff, expressly, $S_f = V_{bound} = 0$. Obviously, the blade creates one degree of freedom, $S_e=0$. Finally, the revolving inertia J_{whole} is the stiffness frame of a whole blade.

The rotating inertia J_{whole} shows a derivative causality as rotational speed is specified with bond I . Literally, blades exhibit the torque as output; its necessities the rotational speed as input. Furthermore, bond I needs a connection alongside the hub. An abridged bond graph shape of a ductile blade is seen in Figure 7.

2.1.3. Pitching system

Each model of pitching procedure is able to be created as a second order system:

$$\omega_n^2 \theta_{ref} = \ddot{\theta} + 2\xi\dot{\theta} + \omega_n^2 \theta \tag{6}$$

whith θ_{ref} , ω_d , and ξ denote standard of pitch angle, natural frequency, and damping ratio, respectively. In (6) can be described as the mass spring damper system, shown in Figure 8. This systema are able to change into bond graph configuration that is seen Figure 9 with an appropriate quantity, namely.

$$F = \theta_{ref} \quad M = 1/\omega_n^2 \quad D = 2\xi/\omega_n \quad K = 1.$$

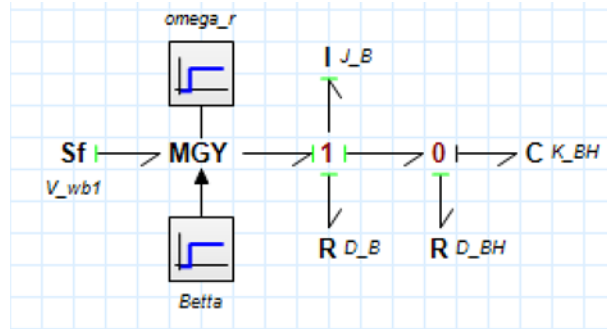


Figure 7. Bond graph shape of turbine blade

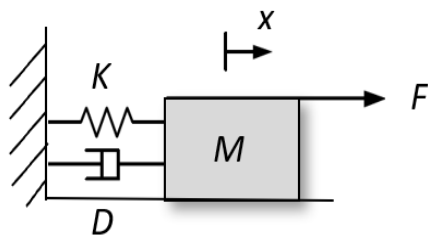


Figure 8. Mass spring damper system

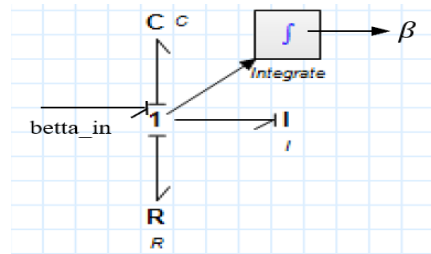


Figure 9. Bond graph of pitching system

2.2. Gearbox model

Wind turbine usually has three-stages of gearbox, such as a planetary stage and two more parallel stages which is used for increasing the bifurcate speed. Simplest method to reproduce the gearbox is as a complete form; therefore, the adaptation ratio, N_p/N_g , (N_p denotes the teeth quantity of pinion and N_p describes the teeth quantity of gears) can be familiarized precisely in a transformer. Though, the gearbox is the most significant portions because of its involved dynamics of wind turbine. Consequently, a more detailed form desires to be established. Coudert *et al.* [27], Luo and Di [28] a thorough gearbox based on Bond graph method is offered.

Figure 10 shows the gearbox scheme. In the gearbox model some concerns can be allowed for possibility, namely ring gear is a static stage, individual one parallel juncture is counted; carrier is looked on as input and sun becomes the output. Mesh stiffness among planet ring and planet sun is taken into consideration, and bearing stiffness are ignored.

The model of Figure 11 describes the planet gears denoted by energy of torpidity, J_{pi} ($i = 1, 2, 3$). The planet gears are adjoined to sun gear and ring gear through the lattice rigidity, K_{sp} and K_{rp} , respectively. A connection among lattice rigidity and carrier gear is created. The energy of torpidity J_r (ring gear) possess a derivative causality because of a fixed ring stage concern; this denotes a $S_f = 0$ source is constrained (at the 1_s junction) with the purpose of taking an advantage of a bifurcate speed of planetary gearbox. On this structure, Z_i ($i = p, s, r$) characterizes the teeth quantity of every gear. The output of sun gear is attached to TF part and denoting the two parallel steps output. A scheme of the gearbox utilizing the parameter assessment construct created in [29].

The flow junction $I_{1 \rightarrow 3}$, I_4 , I_5 , I_6 describe the rotational speed of planets gear, carrier gear, ring gear, and sun gear, respectively. Both of them associated to every one through TF parts. Recognizing a planet 1 revealed that a zero junction 0_1 , among the transformer TF_1 , TF_2 , and TF_3 , that characterizes the planet shifts in tangential direction and becomes an effort variable. Moreover, the mesh stiffness among planet gear and sun gear is merged. Transformers $TF_1: Z_s$, $TF_2: 1/Z_s$, and $TF_3: Z_p$ are able to create the rotating speed of the sun gear, the linear velocity of the planet rotation around the sun gear, and the planet auto-rotation. Moreover, Z_s is quantity of sun gear teeth, Z_r is quantity of ring gear teeth, and Z_p is quantity of planet gear teeth. The structure is similar to zero junction 0_2 , but respecting a link among planet gear, ring gear, and carrier gear.

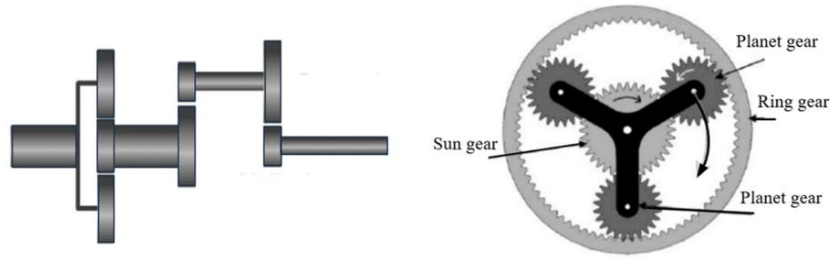


Figure 10. Gearbox wind turbine scheme

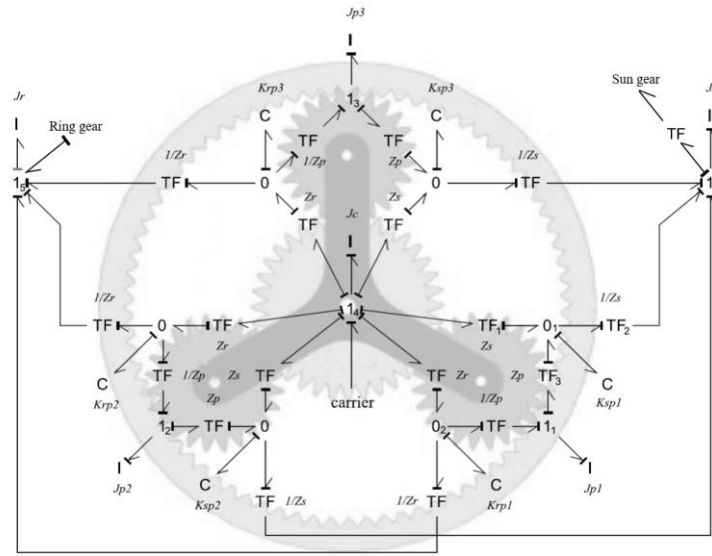


Figure 11. Bond graph model of planetary gear [30]

2.3. Tower model

A drawing of wind turbine system is seen in Figure 12 by ram force performing along the construction. A tower motion is supposed not possess an effect on mechanical scheme but influenced only on its input. Dynamic calculation of tower movement is able to describe by way of:

$$m_t \frac{d^2}{dt^2} Z = F_t - D_t \frac{d}{dt} Z - K_t Z \tag{7}$$

where m_t , K_t , F_t , and D_t are tower mass, tower stiffness, wind force on tower and tower damping, respectively.

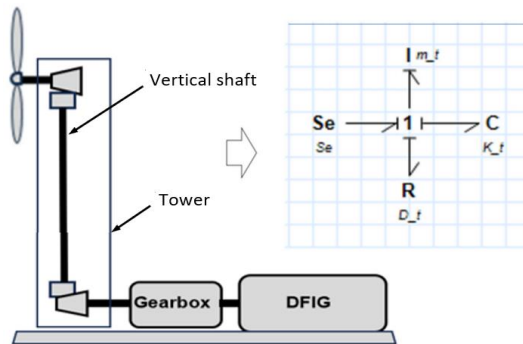


Figure 12. Pictorial of wind turbine and shortened bond graph of tower movement

2.4. Doubly-fed induction generator model

Typically, in an asynchronous generator, namely a doubly-fed induction generator, the three kinds of energy ports are stator, rotor, and the shaft, shown in Figure 13. Stator picks-up the energy transfer from mains; rotor possibly will be delivered by electric energy from mains just like a doubly-fed induction generator or allocates its energy with stator with respect to squirrel cage induction generator. The shaft delivers mechanical energy to attached load. Exchange of energy between three ports appears in an air gap.

Mathematical model of a three-phase induction generator is usually made by fifth order nonlinear differential equalities [31]. Karnopp [32] suggests a bond graph structure describing the particular equations. Models can be represented using a Park reference of frame. The assumption considered for the induction generator model that allocated inductances among armature, *amortisseur* wiring, and field on *d*-axis windings are identical is foundation of conservative concept of the machine structure. Winding losses and rotor slots are disregard; the latitudinal distribution of stator fluxes and opening wave are sinusoidal shapes. The *amortisseur* wiring that are located adjacent air-gap exhibit flux connecting *amortisseur* wiring whose amount is equivalent to flux relating frame. A casual *dq0*-casing revolving close a homopolar *0*-axis to the velocity ω_s is selected.

Figure 14 describes the following items:

- i) Stator phase coils, *a*, *b*, and *c* with i_a, i_b, i_c are the stator phase currents; v_a, v_b, v_c are the stator phase voltages, r_a, r_b, r_c are the stator phase resistances and L_a, L_b, L_c are the stator phase self-inductances.
- ii) Field coils with i_F and v_F represent the field current and voltage, respectively; r_F is the field resistance and L_F is the field self-inductance.
- iii) The direct-axis damping coils with i_D and v_D represent the damping current and voltage on the *d*-axis, respectively; r_D and L_D are the damping resistance and self-inductance on the *d*-axis, respectively.
- iv) The quadrature-axis damping coils with i_Q and v_Q represent the damping current and voltage on the *q*-axis, respectively; r_Q and L_Q are the damping resistance and self-inductance on the *q*-axis, respectively.

Figure 14 represents doubly-fed induction generator with six magnetically joined coils which working by rotor position. The instantaneous voltage of every coil has a shape like;

$$v = \pm \sum ri \pm \lambda \tag{8}$$

with λ , r , and i describe flux linkage, coil resistance and stator currents running from generator ports, respectively. An impressive shortening in the mathematical portrayal of the induction generator is attained from the Park's transformation. The Park's transformation converts quantities of completely stator phases *a*, *b* and *c* into recent parameters of reference frame of which rotates with rotor. Consequently, through description;

$$i_{dq0} = P i_{abc} \tag{9}$$

where the current vectors are expressed as,

$$i_{dq0} = [i_d \ i_q \ i_0]^T \quad i_{abc} = [i_a \ i_b \ i_c]^T \tag{10}$$

Park's transformation is;

$$P = \sqrt{\frac{2}{3}} \begin{bmatrix} \frac{1}{\sqrt{2}} & \frac{1}{\sqrt{2}} & \frac{1}{\sqrt{2}} \\ \cos \theta & \cos(\theta - 2\pi/3) & \cos(\theta + 2\pi/3) \\ \sin \theta & \sin(\theta - 2\pi/3) & \sin(\theta + 2\pi/3) \end{bmatrix} \tag{11}$$

The angle between axis of stator revolving magnetic field and rotor is specified through;

$$\theta = \omega_r t + \delta + \pi/2 \tag{12}$$

with ω_r denotes valued angular frequency (in rad/s) and δ denotes angle of synchronous torque (in electrical radian). Correspondingly, to convert voltages and flux linkages;

$$v_{dq0} = P v_{abc} \quad \lambda_{dq0} = P \lambda_{abc} \tag{13}$$



Figure 13. Doubly-fed induction generator 2.5 kW 220/380 V

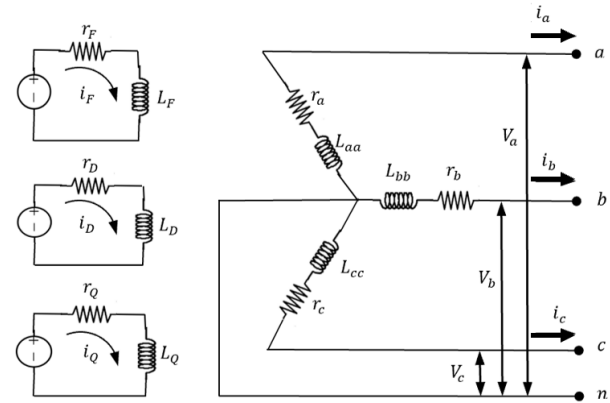


Figure 14. Schematic diagram of doubly-fed induction generator

In Figure 15, T_m denotes mechanical torque, J_G is moment of inertia, D_G is damper constant, $I: M_{dD}$ and $I: M_{qQ}$ are the magnetic coupling among self and mutual inductances of coils on d -axis and on q -axis, respectively. Four modulated sources which fixed on ω_s is virtual sources, because power sum is equal to zero and are only a mathematical corollary of the form. Because of every generator is connected into rotor, stator does not affect by the rotor velocity.

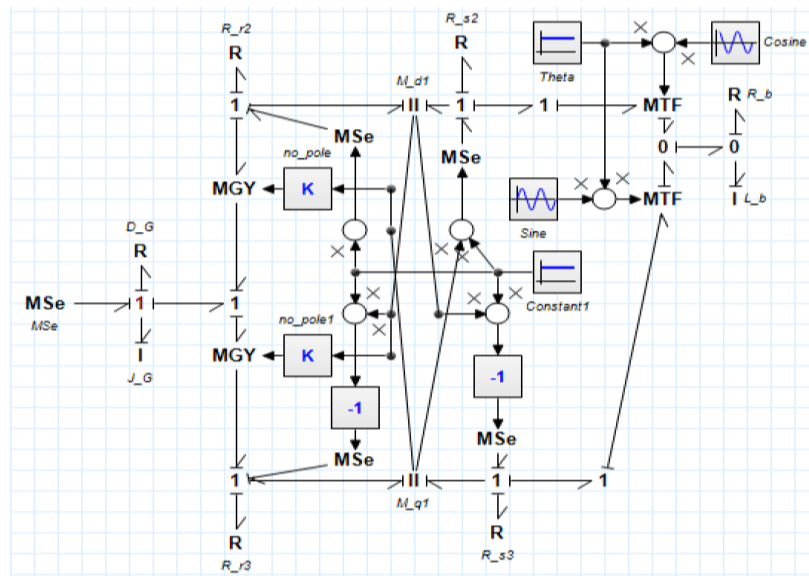


Figure 15. Doubly-fed induction generator-based bond graph scheme

3. RESULTS AND DISCUSSION

Through taking the place of the succeeding numerical amounts of the variables: $J_r = 0.562$, $D_a = 1.05$, $r_f = 0.0742$, $r_D = 6.95$, $r_Q = 0.054$, $L_q = 0.04$, $L_Q = 0.061$, $L_f = 0.036$, $r_b = 0.0014$, and $L_B = 0.0045$ into Figure 15, the steady-state condition of DFIG is achieved [33], [34]. The wind speed v_w , such as 2 m/s, is an input and is utilized to compute the wind turbine torque (T_a). Mechanical torque, T_m , and electromechanical torque, T_{em} , arrival from generator is in opposition and this create a rotation speed relating to angular speed of the rotor. For simulation, a step input is applied as the angular speed of rotating blade. For the purpose of proving the conducting of steady state circumstance of proposed configuration, wind turbine simulation utilizing a 20-Sim software with prearranged numerical values is presented. Bond graph configuration is seen in Figure 16.

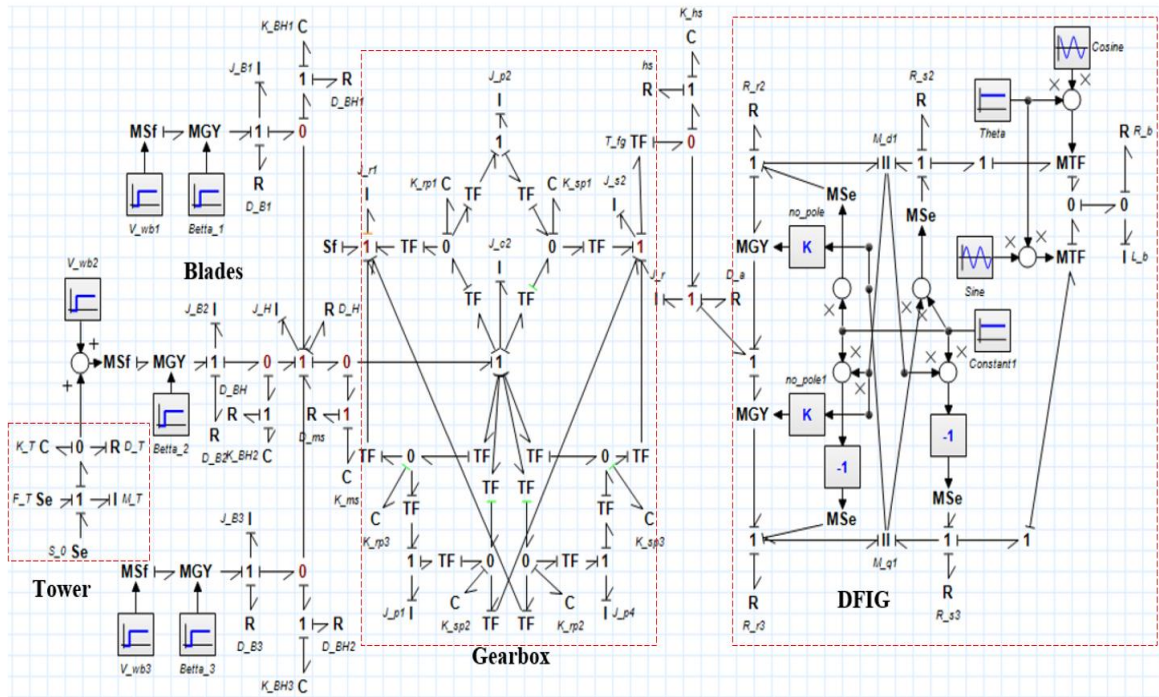


Figure 16. Wind turbine-based bond graph scheme with derivative causality assignment in 20-Sim

The simulation scenario for the constant wind (namely 2 m/s) is shown in Figure 17. With the diameter of blade of 3 m, the value of the hub speed is almost 1.33 rad/s. The velocity in generator rises proportionally with the wind speed. Velocity of generator reaches its nominal value (157.08 rad/s) because of the steady-state condition of generator is achieved at 5.6 second.

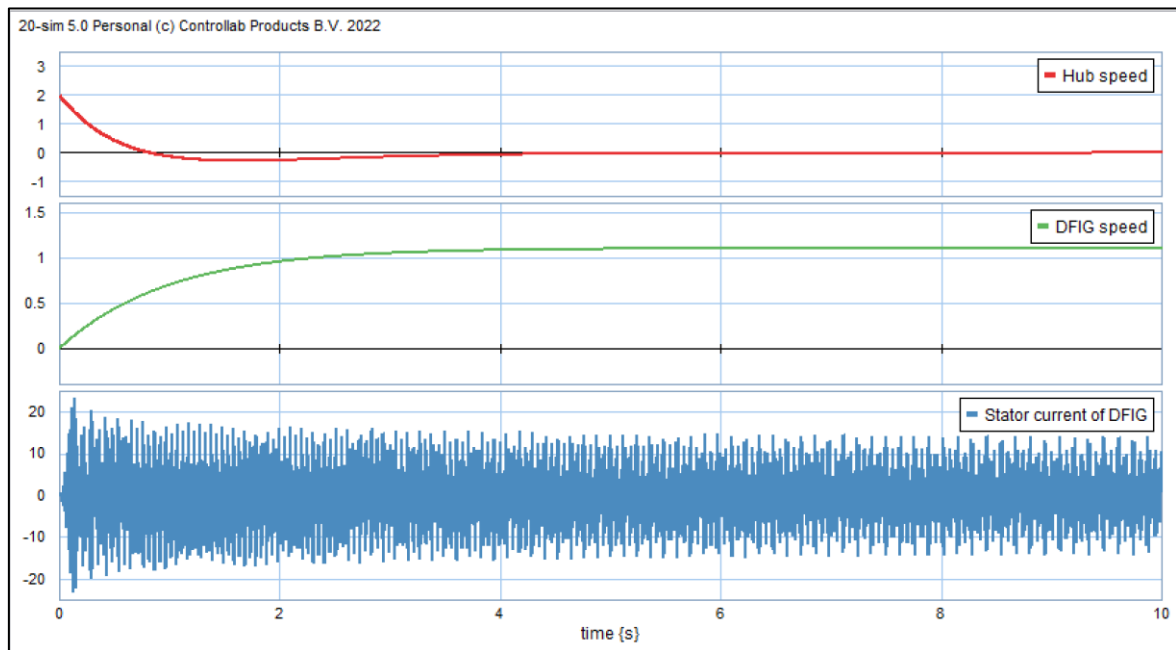


Figure 17. Constant wind responses: hub speed, torque speed, and stator current

In reality the wind is a stochastic parameter of wavering nature, the next simulation was performed by variable wind velocity as seen in Figure 18. Figure 18 also schematizes behavior of simulation for the designated wind turbine parameters, namely hub, gearbox, and doubly-fed induction generator. When wind speed varies at the nominal value (1.33 rad/s) and standard deviation of 1 rad/s for long periods, the generator speed still reaches its nominal value.

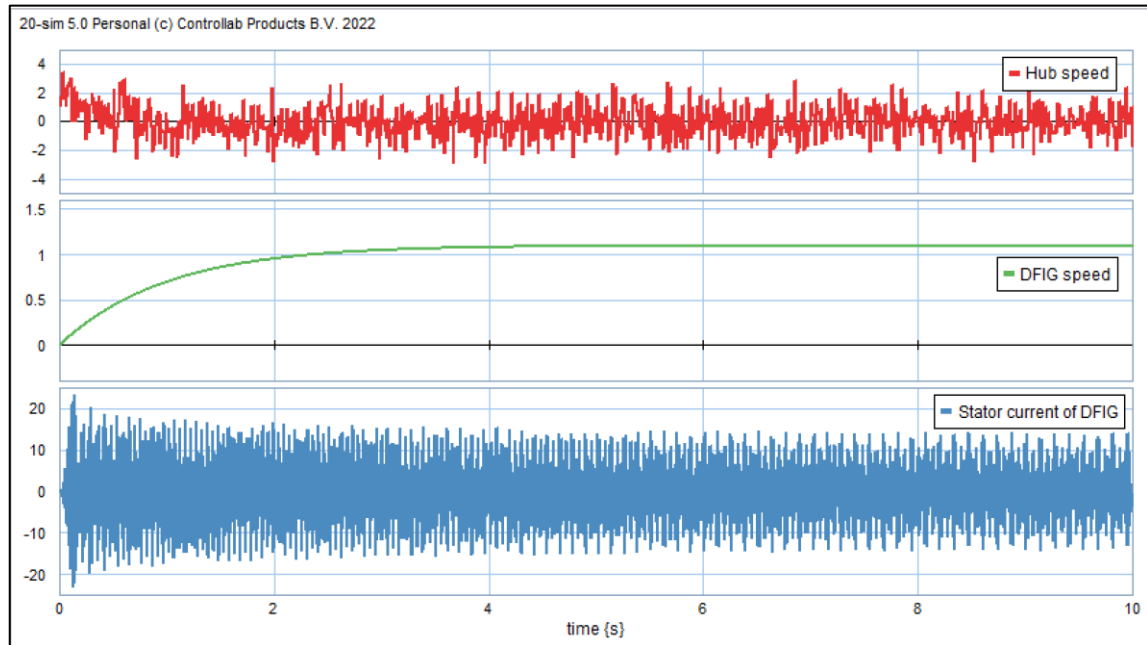


Figure 18. Variable wind responses: hub speed, gearbox speed, and stator current

4. CONCLUSION

This paper has been dedicated to model a variable wind turbine utilizing bond graph procedure. The suppleness has been set up into blades, hub and tower; a comprehensive configure expressing character of all the important parts of the structure is achieved with less effort competed with else approaches. With the purpose of utilizing an aerodynamic force, blade construction is thought have being elastic figure. The nonlinear configuration of wind turbine comprised of gearbox, pitching structure, tower, and doubly-fed induction generator. Modelling dynamic structure in the conventional way and bond graph method is quite different, but the result is a model with accurately the same prevailing equations. It is also conformed to; bond graph procedure offers superior interpretation of what occurred in the system. This study can be furthered by potentials that can contribute to enhance the complete wind conversion sequence. Between the possible prospects are a model of converters utilizing the bond graph procedure. And also, an improvement active and reactive power control approaches on doubly-fed induction generator using power converters-based bond graph scheme.

ACKNOWLEDGEMENTS

This work has been fully funded by DRTPM, Kemendikbudristek, Republik Indonesia, under Grant no. 181/E5/PG.02.00.PL/2023, no. 0423.25/LL5-INT/AL.04/ 2023, and no. 03/ITNY/LPPMI/Pen.DRTPM/PFR/VII/2023.

REFERENCES

- [1] IRENA, "The costs of financing for renewable energy in 2023," International Renewable Energy Agency Abu Dhabi, United Arab Emirates, 2023.
- [2] REN21, "Renewables 2023 global status report," in *Renewable Energy Policy Network for the 21st Century (REN21)*, Paris, France, 2023.
- [3] M. Farghali *et al.*, "Social, environmental, and economic consequences of integrating renewable energies in the electricity sector: a review," *Environmental Chemistry Letters*, vol. 21, no. 3, pp. 1381–1418, Mar. 2023, doi: 10.1007/s10311-023-01587-1.

- [4] K. K. Jaiswal *et al.*, “Renewable and sustainable clean energy development and impact on social, economic, and environmental health,” *Energy Nexus*, vol. 7, p. 100118, Sep. 2022, doi: 10.1016/j.nexus.2022.100118.
- [5] T. Z. Ang, M. Salem, M. Kamarol, H. S. Das, M. A. Nazari, and N. Prabakaran, “A comprehensive study of renewable energy sources: classifications, challenges and suggestions,” *Energy Strategy Reviews*, vol. 43, p. 100939, Sep. 2022, doi: 10.1016/j.esr.2022.100939.
- [6] A. G. Olabi *et al.*, “Wind energy contribution to the sustainable development goals: case study on London array,” *Sustainability (Switzerland)*, vol. 15, no. 5, p. 4641, Mar. 2023, doi: 10.3390/su15054641.
- [7] Y. Vidal, L. Acho, N. Luo, M. Zapateiro, and F. Pozo, “Power control design for variable-speed wind turbines,” *Energies*, vol. 5, no. 8, pp. 3033–3050, Aug. 2012, doi: 10.3390/en5083033.
- [8] A. Afkari, F. E. Z. Lamzouri, and E. M. Boufounas, “A robust controller for a variable-speed wind turbine using a single mass model,” *E3S Web of Conferences*, vol. 297, p. 1042, 2021, doi: 10.1051/e3sconf/202129701042.
- [9] B. Boukhezzar and H. Siguerdidjane, “Nonlinear control of a variable-speed wind turbine using a two-mass model,” *IEEE Transactions on Energy Conversion*, vol. 26, no. 1, pp. 149–162, Mar. 2011, doi: 10.1109/TEC.2010.2090155.
- [10] M. Sami and R. J. Patton, “Fault tolerant adaptive sliding mode controller for wind turbine power maximisation,” *IFAC Proceedings Volumes (IFAC-PapersOnline)*, vol. 7, no. PART 1, pp. 499–504, 2012, doi: 10.3182/20120620-3-DK-2025.00144.
- [11] M. Martins, A. Perdana, P. Ledesma, E. Agneholm, and O. Carlson, “Validation of fixed speed wind turbine dynamic models with measured data,” *Renewable Energy*, vol. 32, no. 8, pp. 1301–1316, Jul. 2007, doi: 10.1016/j.renene.2006.06.007.
- [12] S. M. Mueen *et al.*, “Comparative study on transient stability analysis of wind turbine generator system using different drive train models,” *IET Renewable Power Generation*, vol. 1, no. 2, pp. 131–141, 2007, doi: 10.1049/iet-rpg:20060030.
- [13] W. Borutzky, “Bond graph based physical systems modelling,” in *Bond Graph Methodology*, Springer London, 2010, pp. 17–88.
- [14] J. Kypuros, “Basic bond graph elements,” in *System Dynamics and Control with Bond Graph Modeling*, Florida, USA: CRC Press Taylor & Francis Group, 2013, p. 36.
- [15] P. C. Breedveld, “Concept-oriented modeling of dynamic behavior,” in *Bond Graph Modelling of Engineering Systems*, Springer New York, 2011, pp. 3–52.
- [16] A. Mohammed, B. Sirahbizu, and H. G. Lemu, “Optimal rotary wind turbine blade modeling with bond graph approach for specific local sites,” *Energies*, vol. 15, no. 18, p. 6858, Sep. 2022, doi: 10.3390/en15186858.
- [17] G. Gonzalez-A, N. Barrera-G, G. Ayala, J. Aaron Padilla, and D. Alvarado-Z, “Dynamic performance of a Skystream wind turbine: A bond graph approach,” *Cogent Engineering*, vol. 6, no. 1, Jan. 2019, doi: 10.1080/23311916.2019.1709361.
- [18] F. C. Mehlan, E. Pedersen, and A. R. Nejad, “Modelling of wind turbine gear stages for digital Twin and real-time virtual sensing using bond graphs,” *Journal of Physics: Conference Series*, vol. 2265, no. 3, p. 32065, May 2022, doi: 10.1088/1742-6596/2265/3/032065.
- [19] C. Fu, K. Lu, Y. D. Xu, Y. Yang, F. S. Gu, and Y. Chen, “Dynamic analysis of geared transmission system for wind turbines with mixed aleatory and epistemic uncertainties,” *Applied Mathematics and Mechanics (English Edition)*, vol. 43, no. 2, pp. 275–294, Jan. 2022, doi: 10.1007/s10483-022-2816-8.
- [20] J. Wu, H. Yan, S. Liu, Y. Zhang, and W. Tan, “Bond graph-based approach to modeling variable-speed gearboxes with multi-type clutches,” *Applied Sciences (Switzerland)*, vol. 12, no. 12, p. 6181, Jun. 2022, doi: 10.3390/app12126181.
- [21] G. H. Geitner and G. Komurgoz, “Key characteristics of generic bond graphs for planetary gears,” *Mechanism and Machine Theory*, vol. 178, p. 105082, Dec. 2022, doi: 10.1016/j.mechmachtheory.2022.105082.
- [22] A. A. Nada and A. S. Al-Shahrani, “Dynamic modelling and experimental validation of small-size wind turbine using flexible multibody approach,” *International Journal of Dynamics and Control*, vol. 5, no. 3, pp. 721–732, Mar. 2017, doi: 10.1007/s40435-016-0241-2.
- [23] S. Agarwal, L. Chalal, G. Dauphin-Tanguy, and X. Guillaud, “Bond graph model of wind turbine blade,” *IFAC Proceedings Volumes*, vol. 45, no. 2, pp. 409–414, 2012, doi: 10.3182/20120215-3-at-3016.00072.
- [24] J. Chen and Q. Wang, “Aerodynamic characteristics of wind turbine airfoils,” in *Wind Turbine Airfoils and Blades, Optimization Design Theory*, Erlin, Boston: De Gruyter: China Science Publishing & Media Ltd., 2018.
- [25] E. Branlard, *Wind Turbine Aerodynamics and Vorticity-Based Methods*, vol. 7. Cham: Springer International Publishing, 2017.
- [26] C. Anderson, “Rotor design and performance,” in *Wind Turbines, Theory and Practice*, Cambridge University Press, 2020, pp. 64–85.
- [27] N. Coudert, G. Dauphin-Tanguy, and A. Rault, “Mechatronic design of an automatic gear box using bond graphs,” in *Proceedings of the IEEE International Conference on Systems, Man and Cybernetics*, 1993, vol. 2, pp. 216–221, doi: 10.1109/icsmc.1993.384873.
- [28] Y. Luo and T. Di, “Dynamics modeling of planetary gear set considering meshing stiffness based on bond graph,” *Procedia Engineering*, vol. 24, pp. 850–855, 2011, doi: 10.1016/j.proeng.2011.11.2749.
- [29] R. F. Ngwompo and S. Scavarda, “Dimensioning problems in system design using bicausal bond graphs,” *Simulation Practice and Theory*, vol. 7, no. 5, pp. 577–587, Dec. 1999, doi: 10.1016/S0928-4869(99)00013-0.
- [30] R. Sanchez and A. Medina, “Wind turbine model simulation: A bond graph approach,” *Simulation Modelling Practice and Theory*, vol. 41, pp. 28–45, Feb. 2014, doi: 10.1016/j.simpat.2013.11.001.
- [31] P. C. Krause, O. Wasynczuk, and S. D. Sudhoff, “Symmetrical induction machine,” in *Analysis of Electric Machinery and Drive Systems 2nd Edition*, USA: IEEE Press, 2002.
- [32] D. C. Karnopp, “Understanding induction motor state equations using bond graph,” in *International Conference on Bond Graph Modeling and Simulation (ICBGM)*, 2003.
- [33] G. Gonzalez-A and O. Barriga, “Analysis of a hydroelectric plant connected to electrical power system in the physical domain,” *International Journal of Electrical, Computer, Energetic, Electronic and Communication Engineering*, vol. 2, no. 7, pp. 1306–1312, 2008.
- [34] H. Dehnavifard, M. A. Khan, and P. Barendse, “Development of a 5kW scaled prototype of a 2.5 MW Doubly-fed induction generator,” in *2015 IEEE Energy Conversion Congress and Exposition, ECCE 2015*, Sep. 2015, pp. 990–996, doi: 10.1109/ECCE.2015.7309796.

BIOGRAPHIES OF AUTHORS

Sugiarto Kadiman    holds the Bachelor degree, Master degree, and Doctor degree in Electrical Engineering from Gadjah Mada University, Yogyakarta, Indonesia, in 1989, 2000, and 2014, respectively. Since 2014, he is working as Associate Professor in the Department of Electrical Engineering, Faculty of Engineering and Planning, Institut Teknologi Nasional Yogyakarta, Yogyakarta, Indonesia, including the Head of Department and Head of Electric Installation Lab. His research interest is model of power system analysis, modelling and simulation systems, and electronic controlled power systems. He does research with grant from DRTPM, Kemendikbudristek, in The Dynamic of Synchronous Generator Under Unbalanced Steady State Operation and Unbalanced Transient Condition, Higher Order Model of Synchronous Generator, and Power System Stabilizer and PID Impacts on Transient condition in synchronous generator. His current project is model development and control design of variable speed wind power plant with DFIG configuration. He can be contacted at email: sugiarto.kadiman@itny.ac.id



Oni Yuliani    received the Bachelor degree in Chemical Engineering from Sriwijaya University, Palembang, Indonesia, in 1996. She received Master degree in Computer Science from Gadjah Mada University, Yogyakarta, Indonesia in 2006. Since 1994, she is working as senior lecturer in the Department of Electrical Engineering, Faculty of Engineering and Planning, Institut Teknologi Nasional Yogyakarta, Yogyakarta, Indonesia, including Head of Department. Her research interest includes computer algorithm and program, and probability and stochastic process. She can be contacted at email: oniyuliani@itny.ac.id.